Electric dipole moments generated by nuclear Schiff moment interactions: A reassessment of the atoms ^{129}Xe and ^{199}Hg and the molecule ^{205}TlF

Mickaël Hubert*
EPITA, 14 Rue Claire Pauilhac, 31000 Toulouse, France

Timo Fleig†
Laboratoire de Chimie et Physique Quantiques, IRSAMC, Université Paul Sabatier Toulouse III, 118 Route de Narbonne, F-31062 Toulouse, France

(Received 15 March 2022; accepted 6 July 2022; published 30 August 2022)

We present relativistic many-body calculations of atomic and molecular Schiff-moment interaction constants including interelectron correlation effects using atomic Gaussian basis sets specifically optimized for the Schiff interaction. Our present best results employing a Gaussian nuclear density function are $\alpha_{\rm SM} = (0.362 \pm 0.025) \times 10^{-17}\,\frac{e\,\mathrm{cm}}{e\,\mathrm{fm}^3}$ for atomic ^{129}Xe, $\alpha_{\rm SM} = (-2.26 \pm 0.23) \times 10^{-17}\,\frac{e\,\mathrm{cm}}{e\,\mathrm{fm}^3}$ for atomic ^{199}Hg, and $W_{\rm SM} = (39\,967 \pm 3600)$ a.u. for the thallium nucleus in the molecule ^{205}TlF. We discuss agreements and discrepancies between our present results and those from earlier calculations on the atoms ^{129}Xe and ^{199}Hg. Using the most recent measurements of $\mathcal{P},\mathcal{T}$-odd electric dipole moments and the present interaction constants, reliable upper bounds on the Schiff moments of the ^{199}Hg and ^{205}Tl nuclei are determined in the context of a single-source assumption.

DOI: 10.1103/PhysRevA.106.022817

I. INTRODUCTION

The standard model (SM) of elementary particle physics [1–3] is an extremely well-tested theory of fundamental particles and their interactions. However, it leaves a number of firmly established observations about our universe unexplained, like its matter and energy content [4]. Specifically, the SM does not allow the accommodation of baryon asymmetry of the universe (BAU), i.e., the significant surplus of denominational matter over antimatter in the universe [5].

A necessary condition for explaining the BAU is the violation of the combined discrete symmetries charge conjugation and parity ($\mathcal{CP}$), favoring the production of a matter over an antimatter particle [6]. $\mathcal{CP}$ violation (CPV) has been observed in the decay of certain mesons [7–9], and a partial theory of $\mathcal{CP}$ violation has become an integral part of the SM [10]. However, it is generally agreed that this manifestation of $\mathcal{CP}$ violation is insufficient for explaining the BAU. New sources of $\mathcal{CP}$ violation are hence required, which in particular generally also yield flavor-diagonal $\mathcal{CP}$ violation [11]. Under the assumption that $\mathcal{CPT}$ invariance ($\mathcal{T}$ denoting time reversal) of fundamental physical laws holds [12], CPV implies the violation of $\mathcal{T}$ symmetry. The detection of an atomic or molecular electric dipole moment (EDM), the Hamiltonian of which is $\mathcal{P},\mathcal{T}$-odd, would in turn indicate CPV. The SM CPV phases [10,13] give rise to EDMs many orders of magnitude below the current experimental limits (see Ref. [14] and references therein), which makes EDMs nearly background-free probes of beyond-SM CPV [15].

The origins of nuclear, atomic, and molecular EDMs in terms of fundamental CPV phases may be diverse [16–18]. In electronically closed-shell systems like atomic mercury (Hg) [19] or molecular thallium fluoride (TlF) [20,21] the situation is relatively complicated, and several hadronic mechanisms may contribute to the leading order. The nuclear Schiff moment and the nucleon-electron tensor-pseudotensor interaction are the leading CPV sources at the hadronic and nuclear energy scale in such systems.

The nuclear Schiff potential is a low-order $\mathcal{P},\mathcal{T}$-odd term in the expansion of the nuclear charge distribution [22,23] which polarizes the electron cloud in an atomic system, giving rise to atomic/molecular EDMs. Thus, atomic-scale measurements search for or constrain the nuclear Schiff moment and—in turn—the underlying CPV sources. The chosen systems and states have electronically closed shells which strongly suppress leptonic CPV sources such as the electron EDM d_e and some semileptonic CPV sources such as the nucleon-electron scalar-pseudoscalar coupling C_S [24,25]. The currently most sensitive measurement [26] is $|d_{\rm Hg}| < 7.4 \times 10^{-30} e\,\mathrm{cm}$ with spin-polarized mercury atoms, ^{199}Hg, leading to an upper bound on the Schiff moment of $|S_{\rm Hg}| < 3.1 \times 10^{-13} e\,\mathrm{fm}^3$ (95% C.L.). In the calculation of this upper bound an average over interaction constants from different theory groups has been used. The upper bound translates [19,27,57] into constraints on more fundamental parameters, the CPV pion-nucleon couplings $g_\pi^{(0)}$, $g_\pi^{(1)}$, and $g_\pi^{(2)}$; the nucleon EDMs d_p and d_n; the quantum chromodynamics Θ parameter; and chromo-EDMs.

In the present paper we pursue several goals.

(i) The Schiff moment interaction in general is quite strongly dependent on the quality of the atomic basis set for the target nucleus in electronic-structure calculations, as

*mickael.hubert@epita.fr
†timo.fleig@irsamc.ups-tlse.fr

has also been substantiated earlier [28,29]. Our calculations confirm this finding for all systems we have studied so far. In the present paper, we present a systematic approach to extending standard atomic basis sets with the aim of a reliable and economic description of the Schiff moment interaction in both atoms and molecules. In the following section we define our method for calculation of atomic and molecular Schiff moment interactions and give a detailed description of the strategy for optimizing required Gaussian basis sets.

(ii) In Sec. III we discuss applications to ^{129}Xe, ^{199}Hg, and ^{205}TlF using a large optimized basis set for each respective system and carefully taking into account interelectron correlation effects shellwise and at various excitation ranks. Based on our findings we address current disagreements among previously published results for atomic Schiff moment interactions in ^{129}Xe and ^{199}Hg.

(iii) We conclude on our study in Sec. IV and use the most recent experimental EDM measurements [26,30] and our calculated interaction constants for these systems to derive constraints on the respective nuclear Schiff moments.

II. THEORY AND METHODS

A. Theory

1. The atomic Schiff moment interaction Hamiltonian

The atomic Schiff moment interaction for a single electron in the field of a point nucleus has been given as [see Ref. [22], Eq. (8.75)]

$$\hat{H}_{\mathrm{SM}} = -e\mathbf{S}\cdot\nabla_r\delta(\mathbf{r}), \tag{1}$$

where the vector coefficient $\mathbf{S} := S\frac{\mathbf{I}}{I}$ is the Schiff moment [31] of the nucleus with $\mathbf{I}$ denoting nuclear spin and S the scalar Schiff moment constant [32].

Recent developments use a more realistic finite nuclear charge density, and the Hamiltonian for the interaction of an electron with the Schiff potential [32] has been represented as

$$\hat{H}_{\mathrm{SM}} = -e\varphi_{\mathrm{SM}}(\mathbf{r}) = -3e\,\frac{\mathbf{S}\cdot\hat{\mathbf{r}}}{B}\rho(\mathbf{r}), \tag{2}$$

where $B = \int_0^\infty \rho(\mathbf{r})r^4dr$, and $\rho(\mathbf{r})$ is the nuclear charge density at position $\mathbf{r}$.

2. Expectation value approach to Schiff moment interaction

Our principal strategy is to determine the E-field-dependent $\mathcal{P},\mathcal{T}$-odd energy shift $\Delta\varepsilon$ as a function of an atomic interaction constant. The full details of the general approach are found in Ref. [33]. Here, we present the specific approach for the calculation of Schiff moment interaction constants.

a. Atoms. For atomic calculations we include an external homogeneous electric field E_{ext} along the z axis. In an atom with n electrons the associated $\mathcal{P},\mathcal{T}$-odd energy shift can then be expressed as an expectation value over the one-electron Hamiltonian in Eq. (2) (here in a.u.):

$$\Delta\varepsilon_{\mathrm{SM}} = -S_z\frac{3}{B}\left\langle\sum_{j=1}^{n}\hat{z}_j\,\rho(\mathbf{r}_j)\right\rangle_{\psi(E_{\mathrm{ext}})}, \tag{3}$$

where $\psi(E_{\mathrm{ext}})$ is the electronic wave function of the field-dependent state. We first solve a zeroth-order problem,

$$\hat{H}(E_{\mathrm{ext}})|\psi(E_{\mathrm{ext}})\rangle = \varepsilon(E_{\mathrm{ext}})|\psi(E_{\mathrm{ext}})\rangle, \tag{4}$$

with ε being the field-dependent energy eigenvalue and $\hat{H}(E_{\mathrm{ext}})$ the Dirac-Coulomb Hamiltonian including the interaction term with the external field:

$$\begin{aligned}\hat{H}(E_{\mathrm{ext}}) &:= \hat{H}^{\text{Dirac-Coulomb}} + \hat{H}^{\text{Int-Dipole}}\\ &= \sum_j^n\left[c\,\boldsymbol{\alpha}_j\cdot\mathbf{p}_j + \beta_j c^2 - \frac{Z}{r_{jK}}\mathbb{1}_4\right]\\ &\quad + \sum_{k>j}^{n}\frac{1}{r_{jk}}\mathbb{1}_4 + \sum_j\mathbf{r}_j\cdot\mathbf{E}_{\mathrm{ext}}\,\mathbb{1}_4.\end{aligned} \tag{5}$$

$\mathbf{E}_{\mathrm{ext}}$ is weak (see below for details) and homogeneous, the indices j and k run over n electrons, Z is the proton number with the nucleus K placed at the origin, and $\boldsymbol{\alpha}$ and β are standard Dirac matrices. E_{ext} is not treated as a perturbation but is included *a priori* in the variational optimization of the wave function, $\psi(E_{\mathrm{ext}})$.

Technically, $\psi(E_{\mathrm{ext}})$ is a configuration interaction (CI) vector [34] built from Slater determinants over field-dependent four-spinors. In the atomic case the wave function is expanded as follows:

$$\psi(E_{\mathrm{ext}}) \mathrel{\widehat{=}} |M_J\rangle = \sum_{I=1}^{\dim\mathcal{F}^t(M,n)} c_{(M_J),I}\,(\mathcal{S}\overline{\mathcal{T}})_{(M_J),I}|\,\rangle, \tag{6}$$

where $|\,\rangle$ is the true vacuum state, $\mathcal{F}^t(M,n)$ is the symmetry-restricted sector of the Fock space (M_J subspace) with n electrons in M four-spinors, $\mathcal{S} = a_i^\dagger a_j^\dagger a_k^\dagger\ldots$ is a string of spinor creation operators, and $\overline{\mathcal{T}} = a_{\bar{l}}^\dagger a_{\bar{m}}^\dagger a_{\bar{n}}^\dagger\ldots$ is a string of creation operators of time-reversal transformed spinors. The determinant expansion coefficients $c_{(M_J),I}$ are generally obtained as described in Refs. [35,36].

The electric dipole moment of the atomic system in terms of the Schiff moment is

$$d_a = \alpha_{\mathrm{SM}}S_z, \tag{7}$$

where using Eqs. (3) and (7) we define the Schiff moment interaction constant as

$$\alpha_{\mathrm{SM}} := \frac{\Delta\varepsilon_{\mathrm{SM}}}{S_z\,E_{\mathrm{ext}}} = \frac{-\frac{3}{B}\left\langle\sum_{j=1}^{n}\hat{z}_j\rho(\mathbf{r}_j)\right\rangle_{\psi(E_{\mathrm{ext}})}}{E_{\mathrm{ext}}}. \tag{8}$$

In the linear régime, $W_a(\psi(E_{\mathrm{ext}})) := -\frac{3}{B}\langle\hat{z}\rho(\mathbf{r})\rangle_{\psi(E_{\mathrm{ext}})} = C\,E_{\mathrm{ext}}$, where C is a constant with respect to E_{ext}. From this it follows that in the linear régime $\alpha_{\mathrm{SM}} = C$, which is independent of E_{ext}. Through numerical analysis we determine the quasilinearity of W_a for $E_{\mathrm{ext}} = 0.0003$ a.u. in the case of Xe and for $E_{\mathrm{ext}} = 0.000\,24$ a.u. in the case of Hg. E_{ext} is oriented along the z axis in the atomic case.

b. Molecules. In the molecular case the unperturbed wave function ψ is not a $\mathcal{P}$ eigenstate; thus no external electric field needs to be applied. The general strategy is similar to the one for atoms but with some modifications. The energy shift is

written as

$$\Delta\varepsilon_{\rm SM} = -S_z \frac{3}{B}\left\langle \sum_{j=1}^{n} \hat{z}_j \rho(\mathbf{r}_j)\right\rangle_{\psi} \tag{9}$$

and the wave function is obtained from the zeroth-order problem

$$\hat{H}|\psi\rangle = \varepsilon|\psi\rangle, \tag{10}$$

with

$$\begin{aligned}\hat{H} &:= \hat{H}^{\text{Dirac-Coulomb}} \\ &= \sum_{j}^{n}\left[c\,\boldsymbol{\alpha}_j\cdot\mathbf{p}_j + \beta_j c^2 - \sum_{K}^{2}\frac{Z_K}{r_{jK}}\mathbb{1}_4\right] \\ &\quad + \sum_{k>j}^{n}\frac{1}{r_{jk}}\mathbb{1}_4 + V_{KL}\end{aligned} \tag{11}$$

for a diatomic molecule where K runs over nuclei and V_{KL} is the classical electrostatic potential energy for the two Born-Oppenheimer-fixed nuclei. The CI expansion of the electronic wave function reads

$$\psi \mathrel{\widehat{=}} |\Omega\rangle = \sum_{I=1}^{\dim\mathcal{F}^t(M,n)} c_{(\Omega),I}\,(\mathcal{S}\overline{\mathcal{T}})_{(\Omega),I}|\,\rangle, \tag{12}$$

where Ω is the total angular momentum projection. The Schiff moment interaction constant for a target nucleus A of a molecule is then written as

$$W_{\rm SM}(A) := \frac{\Delta\varepsilon_{\rm SM}(A)}{S_z(A)} = -\frac{3}{B}\left\langle \sum_{j=1}^{n}\hat{z}_j\rho_A(\mathbf{r}_j)\right\rangle_{\psi}. \tag{13}$$

In practical applications the target nucleus is placed at the origin of the reference frame.

B. Methods

1. Nuclear charge density

To describe the charge density, $\rho(\mathbf{r})$, at position $\mathbf{r}$ for a nucleus with Z protons, we in the present work use a Gaussian model [37] with

$$\rho(\mathbf{r}) = Z\left(\frac{\zeta}{\pi}\right)^{\frac{3}{2}} e^{-\zeta\mathbf{r}^2}, \tag{14}$$

where the exponent ζ is taken from Ref. [37]. This density is used both for the calculation of the electronic wave function and for the evaluation of the interaction constants in Eqs. (8) and (13).

2. Matrix elements

We here present the main ideas of the Schiff moment interaction operator implementation. In a Gaussian nuclear model the prefactor B introduced in Eq. (2) can be written in terms of the parameter ζ from Eq. (14). Integration by parts leads to

$$B = \frac{3}{8\pi\zeta}. \tag{15}$$

The electronic spinors constituting the wave function ψ in Eqs. (8) and (13) are expanded as a linear combination of primitive Gaussians in the DIRAC code. It is, therefore, convenient to contract with the exponential $e^{-\zeta\mathbf{r}^2}$ from Eq. (14) by adding ζ to the primitive Gaussian exponents. Then, the matrix elements to be evaluated in Eqs. (8) and (13) can be written as

$$\langle\psi|e^{-\zeta\mathbf{r}^2}\hat{z}|\psi\rangle = \langle\psi_\zeta|\hat{z}|\psi\rangle, \tag{16}$$

where $\psi_\zeta = \psi e^{-\zeta\mathbf{r}^2}$. Finally, the right-hand side of Eq. (16) is evaluated as a dipole length integral in the DIRAC package.

TABLE I. Atomic Schiff moment interaction constant for Xe calculated at the Hartree-Fock level including core contribution with Gaussian nuclear density [37] for studying electronic-basis-set convergence. $E_{\rm ext}$ is set to 0.0003 a.u. Augmented basis sets are built from Dyall's QZ set including diffuse and correlating functions. We compare with literature results which bear the closest theoretical resemblance to our approach, i.e., perturbed Dirac-Fock theory.

Model	$\alpha_{\rm SM}$ ($10^{-17}\frac{e\,\text{cm}}{e\,\text{fm}^3}$)	$\varepsilon_{\rm DCHF}$ (a.u.)
DZ-21s15p	−1.220	−7446.876435682
TZ-29s22p	−0.379	−7446.895053545
QZ-34s28p	0.318	−7446.895409376
sp-densified QZ-67s55p	0.314	−7446.895379750
sp-densified+1*sp* QZ-69s57p	0.373	−7446.895401869
sp-densified+2*sp* QZ-71s59p	0.375	−7446.895401810
sp-densified+3*sp* QZ-73s61p	0.375	−7446.895401761
sp-densified+4*sp* QZ-75s63p	0.375	−7446.895401779
Double *sp*-densified QZ-133s109p	0.362	−7446.895392349
Double *sp*-densified+3*sp* QZ-139s115p	0.369	−7446.895401848
Dzuba *et al.* [32] (RPA, 2002)	0.38	–
Ramachandran and Latha [43] (CPHF, 2014)	0.374	–
Sakurai *et al.* [44] (CPDF, 2019)	0.38	–

3. Atomic basis sets

The nuclear Schiff moment gives rise to an asymmetric charge distribution on the nuclear surface and a related constant electric field inside the nucleus [31] that is oriented along the nuclear spin **I**. The atomic Schiff moment interaction will, therefore, predominantly affect atomic electronic wave functions that penetrate the atomic nucleus. Equation (2) shows that the Schiff moment interaction is $\mathcal{P}$- and $\mathcal{T}$-violating, thus leading to a mixing of states with opposite parity and, therefore, predominantly to mixing of electronic s and p waves.

Our first goal was to investigate the performance of the standard systematic N-tuple-zeta series of Gaussian basis sets in calculating the Schiff moment interaction constant $\alpha_{\rm SM}$ in Dirac-Coulomb Hartree-Fock (DCHF) approximation. The results in Table I demonstrate that $N = 4$ is a minimal requirement for quantitatively reliable results. Still, compared to the literature results that agree well in mean-field approximation, a standard QZ basis set yields a too small result. Gaussian basis sets of quintuple-zeta (and higher) quality are currently not available for heavy atoms and are time-consuming to develop [38]. Given the physical nature of the Schiff moment interaction it is, therefore, as an alternative, strongly suggested to

increase the s and p subspaces of the most extensive standard Gaussian basis set in order to obtain an accurate description of the relevant matrix elements, written generically as

$$\langle s| - \frac{3}{B}\hat{z}\rho(\mathbf{r})|p\rangle. \tag{17}$$

The strategy of our present basis-set optimization starts from Dyall's relativistic Gaussian basis set, QZ, extended with diffuse and correlating functions [39]. This set is then further augmented taking two criteria into account.

(i) Densification in the s and p spaces. Following the so-called "even-tempered prescription" (see Ref. [40]) we insert a Gaussian function between each adjacent pair of original ones according to

$$\zeta_n = \sqrt{\zeta_{n-1}\,\zeta_{n+1}}, \tag{18}$$

where ζ_i is the exponent in $e^{-\zeta_i \mathbf{r}^2}$ of the ith Gaussian function and $\zeta_{n-1}(\zeta_{n+1})$ is the next larger (smaller) exponent. This procedure could in principle be repeated several times, but the rapid increase in dimension of the s and p spaces leads to a steep increase in computational cost.

(ii) Addition of sp pair(s) of even-tempered dense and diffuse functions. In order to obtain a more extended basis set in a balanced way, we add a pair of Gaussian functions—one diffuse and one dense—to the respective densified basis set. The new compact exponent ζ_{n+1} is obtained according to

$$\zeta_{n+1} = \frac{\zeta_n^2}{\zeta_{n-1}}, \tag{19}$$

where ζ_n and ζ_{n-1} are the two most compact coefficients in the sp-densified basis set defined in the latter point (i).

The new diffuse exponent is obtained accordingly:

$$\zeta_{n-1} = \frac{\zeta_n^2}{\zeta_{n+1}}, \tag{20}$$

where ζ_{n-1} is the new more diffuse coefficient and ζ_n and ζ_{n+1} are the two most diffuse coefficients in the sp-densified basis set defined in point (i).

As shown in Table I for Xe neither is the total Dirac-Coulomb Hartree-Fock energy ($\varepsilon_{\mathrm{DCHF}}$) improved (lowered) nor is the Schiff moment interaction constant α_{SM} changed substantially by a second densification if the respective densification is accompanied by the addition of a sufficient number of pairs of even-tempered compact and diffuse functions (respectively, $+1sp$ and $+3sp$ for simple and double densification, see Table VII). For this reason, we densify the original basis set only once. From Tables I, III, and VII and Fig. 1, respectively, we conclude that our accurate and most economic basis set to describe α_{SM} for Xe and Hg is the single sp-densified Dyall's cvQZ+1sp.

Combining the two aforementioned criteria, we propose a systematic method to optimize Gaussian basis sets suited to address the Schiff moment interaction constant α_{SM}. The starting point is an even-tempered (s, p)-space densification. Then, compact and diffuse (s, p) pairs are added until a minimal DCHF energy converged at a level of $\approx 10^{-6}$ a.u. in reached, as is shown in Fig. 1. Under these circumstances α_{SM} shall be considered converged at the DCHF level.

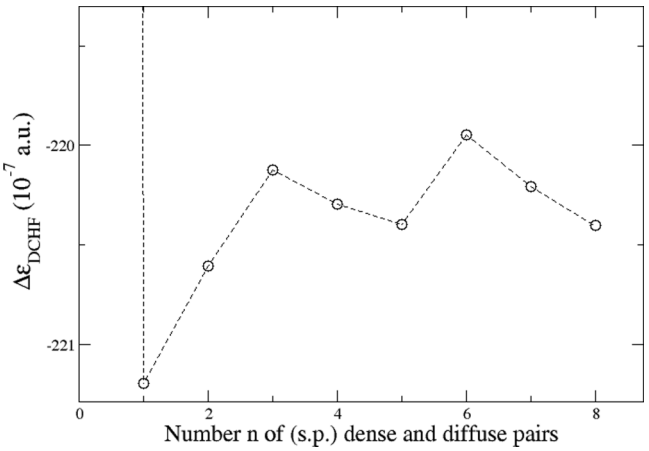

FIG. 1. $\varepsilon_{\mathrm{DCHF}}$ variation from sp-densified QZ for Xe.

4. Molecular basis sets

Obtaining a suitable basis set for a target atom in a diatomic molecule can be achieved by following steps 1 and 2 described in the latter atomic case for the atom with the target nucleus A [see Eq. (13)]. However the basis-set optimization must be done by calculating $\varepsilon_{\mathrm{DCHF}}$ and $W_{\mathrm{SM}}(A)$ in the molecular field. The internuclear distance R is kept fixed during the whole process. It is obtained from experimental data in the present case. For TlF, we conclude from Table V that our accurate and most economic basis set to describe $W_{\mathrm{SM}}(A)$ is the sp-densified Dyall's cvQZ+1sp.

III. RESULTS FOR SCHIFF MOMENT INTERACTION

A. Technical details

All present calculations have been carried out using a locally modified version of the DIRAC program package [41]. The chosen symmetry group is the double-point group C_{2v}^*. Small components of the Dirac spinors are generated through the restricted-kinetic-balance [42] prescription and all small-component integrals are explicitly taken into account.

B. ^{129}Xe

Previous calculations have been carried out in random-phase approximation (RPA) [32] and within the coupled-perturbed Dirac-Hartree-Fock (CPHF) framework [43] yielding very similar results. In recent work using the relativistic normalized coupled-cluster method in singles and doubles approximation (RNCCSD) [44], interelectron correlation effects have been taken into account and a contribution of $\approx -15\%$ to α_{SM} is reported, which is unexpectedly large for Xe. Our general-excitation-rank CI method can test this claim.

In Table II the results from a series of systematic calculations including electron correlation effects from various atomic shells and at various maximum excitation ranks are compiled. As has also been found earlier [45], even the leading correlation effects from the valence shells $(5s, 5p)$, described by double excitations, are weak in the ground state of atomic Xe. In our model SD8 they decrease α_{SM} by only around 6%. The model SDT8 introduces all triple excitations and the model SDTQ_0.2au_SDT8 in addition introduces a subset of quadruple excitations (where the spinor space for

TABLE II. Atomic Schiff moment interaction constant for Xe including electron correlation effects and the core contribution using the Dyall-cvQZ-69s57p basis set and a Gaussian nuclear density [37]. $E_{\rm ext}$ is set to 0.0003 a.u.

CI model/virtual cutoff	$\alpha_{\rm SM}$ ($10^{-17}\frac{e\,\rm cm}{e\,\rm fm^3}$)
DCHF	0.373
SD8/5au	0.348
SD8/10au	0.353
SD8/20au	0.352
SD8/50au	0.352
SDT8/10au	0.351
SDTQ_0.2au_SDT8/10au	0.355
S10_SD18/10au	0.355
S10_SD18/20au	0.359
S10_SD18/50au	0.359
SD10_SD18/20au	0.362
S8_SD16/20au	0.352
S8_SD16/50au	0.353
SD8_SD16/10au	0.355
SD8_SD16/20au	0.352
SD8_SDT16/10au	0.353
S8_SD8_SD24/20au	0.352
Final present	**0.362 ± 0.025**
Dzuba *et al.* [32] (RPA, 2002)	0.38
Dzuba *et al.* [45] (RPA, 2009)	0.38
Ramachandran and Latha [43] (CPHF, 2014)	0.374
Sakurai *et al.* [44] (CPDF, 2019)	0.38
Singh *et al.* [46] (CCSD$_p$T)	0.337
Sakurai *et al.* [44] (RNCCSD, 2019)	0.32 ± 0.002

these quadruples has been truncated at 0.2 a.u.) to the model SD8. Including these higher excitation ranks affects the Schiff interaction constant by less than 1%. Excitations out of the $4d$ shell lead to an increase of about 3%. Here we have not tested higher excitation ranks than doubles since the difference from adding single and double excitations out of the $4d$ shell is already small (around 1%). Finally, the correlation contributions from core shells $3s$, $3p$, $4s$, and $4p$ are seen to be smaller than 1%. Higher-rank core-valence excitations from shells that contribute directly to the Schiff interaction have been taken into account through the model SD8_SDT16 which includes triple excitations from the $5s$ and $5p$ shells as well as triple excitations that are combined singles (doubles) from $4s$ and $4p$ and doubles (singles) from $5s$ and $5p$. Their effect is observed to be smaller than 1% as well.

The final present value is thus calculated as follows. As base value we take the result where the greatest number of electrons has been included in the correlation expansion, from the model S8_SD8_SD24/20au. To this we add corrections due to higher excitation ranks in the valence shells and correlations among and with the $4d$ electrons, according to

$$\begin{aligned}&\alpha_{\rm SM}(\text{Final})\\&\quad=\alpha_{\rm SM}(\text{S8\_SD8\_SD24/20au})\\&\qquad+\alpha_{\rm SM}(\text{SDTQ\_0.2au\_SDT8/10au})-\alpha_{\rm SM}(\text{SD8/10au})\\&\qquad+\alpha_{\rm SM}(\text{SD10\_SD18/20au})-\alpha_{\rm SM}(\text{SD8/20au})\\&\qquad+\alpha_{\rm SM}(\text{SD8\_SDT16/10au})-\alpha_{\rm SM}(\text{SD16/10au}).\end{aligned}$$

TABLE III. Atomic Schiff moment interaction constant for Hg calculated at Hartree-Fock level including core contribution with Gaussian nuclear density [37] for studying electronic-basis-set convergence. $E_{\rm ext}$ is set to 0.000 24 a.u. Augmented basis sets are built from Dyall's QZ set including diffuse and correlating functions.

Model	$\alpha_{\rm SM}$ ($10^{-17}\frac{e\,\rm cm}{e\,\rm fm^3}$)	$\varepsilon_{\rm DCHF}$ (a.u.)
DZ	6.480	−19648.85451859
TZ	−1.267	−19648.89380174
QZ-34s30p	−2.690	−19648.88766826
sp-densified QZ-67s59p	−2.898	−19648.88651484
sp-densified+1*sp* QZ-69s61p	−2.887	−19648.88727782
sp-densified+2*sp* QZ-71s63p	−2.887	−19648.88727627
sp-densified+3*sp* QZ-73s65p	−2.884	−19648.88727625
sp-densified+4*sp* QZ-75s67p	−2.896	−19648.88727630
sp-densified+5*sp* QZ-77s69p	−2.897	−19648.88727619
sp-densified+6*sp* QZ-79s71p	−2.900	−19648.88727624
sp-densified+7*sp* QZ-81s73p	−2.886	−19648.88727628
sp-densified+8*sp* QZ-83s75p	−2.886	−19648.88727631
Dzuba *et al.* [32]	−2.8	–

To this final value we assign an uncertainty of 7% by adding individual uncertainties due to the nuclear density model (3%), the atomic basis set (2%), the higher excitation ranks (1%), and the Breit interaction (1%) that is not present in our Hamiltonian, Eq. (5).

Our final result including the error estimate is not in accord with the coupled-cluster result from Ref. [44]. According to Dzuba [47] correlation contributions beyond the RPA in the case of the Xe atom are not greater than ≈3%. Our final result indeed shows small total correlation effects and is in agreement with the results from Refs. [32,45,46].

C. ^{199}Hg

In Table III we present results of DCHF calculations for the Hg atom and demonstrate their convergence with optimized basis sets, similar to what has been shown in Table I for the Xe atom. Table IV shows correlated results for the mercury atom. Including only single and double excitations for the 12 outermost electrons (shells $5d$ and $6s$) yields a correlation contribution of roughly 10% on top of the DCHF value. This is a significantly greater contribution than the corresponding one in atomic xenon. However, the model SD12 is still not sufficient. Adding full triple excitations to the wave function expansion results in a further 6.5% decrease of $\alpha_{\rm SM}$ on the absolute. Comparing the model SDT12 with the more approximate expansion SD10_SDT12 shows that the effect of three holes in the $5d$ spinor space is rather unimportant (only 0.2% of the DCHF value) and that it is the combined higher excitations out of the $5d$ and $6s$ shells that have to be accounted for. We accomplish this through the model SD10_SDTQ12 where the excitation rank for a maximum of two holes in the $5d$ spinors is maximal. This model yields another 2.4% decrease, on the absolute, at a cutoff of 5 a.u. for the virtual spinors.

Additional effects on $\alpha_{\rm SM}$ from excitations out of the atomic core spinors are accounted for using a virtual cutoff of 20 a.u. We find that one- and two-hole configurations in the $5p$ shell (model SD6_SD18) contribute a mere 0.5%. On the

TABLE IV. Atomic Schiff moment interaction constant for Hg including electron correlation effects and the core contribution using the Dyall-cvQZ-69s61p basis set and a Gaussian nuclear density [37]. E_{ext} is set to 0.000 24 a.u.

Model	α_{SM} ($10^{-17}\frac{e\,\text{cm}}{e\,\text{fm}^3}$)
DCHF	−2.887
SD2/10au	−2.597
SD2/20au	−2.599
SD2/50au	−2.598
SD12/10au	−2.614
SD12/20au	−2.621
SD12/50au	−2.623
SDT12/10au	−2.426
SD10_SDT12/5au	−2.408
SD10_SDT12/10au	−2.420
SD10_SDT12/20au	−2.425
SD10_SDTQ12/5au	−2.339
S6_SD18/20au	−2.599
SD18/20au	−2.608
SD20/10au	−2.568
SD20/20au	−2.590
SD10_SDT20/10au	−2.278
S20_SD32/20au	−2.649
SD32/20au	−2.696
SD34/20au	−2.666
Final present	**−2.26 ± 0.23**
Dzuba *et al.* [45] (CI+MBPT)	−2.6
Latha *et al.* [50] (CCSD, 2015)	−2.46
Singh and Sahoo [51] (CCSD_pT, 2015)	−2.16
Radžiūtė *et al.* [52] (MCDF, 2016)	−2.22
Sahoo and Das [48]	−1.77 ± 0.06

other hand, one- and two-hole configurations in the $4f$ shell (model S20_SD32) contribute about 3%. It is noteworthy that these two corrections are opposed to each other: Excitations out of p shells decrease electron density in p-shell configurations that contribute directly to the generic Schiff moment interaction matrix element in Eq. (17). This leads to an absolute decrease of α_{SM}. On the other hand, excitations out of the f shell reduce the screening of nuclear charge on electrons in directly contributing shells and so lead to an absolute increase of α_{SM}. The same effect can be observed when the $5d$ shell is opened for excitations (model SD12 vs SD2). This interpretation of the physics of correlation effects on the Schiff moment interaction in Hg is confirmed when higher-rank core-valence excitations from atomic shells that contribute directly to this interaction are taken into account, similar to what we have done for Xe above. The model SD10_SDT20 comprises more than 1.6×10^9 Slater determinants and includes full triple excitations from the $5s$, $5p$, and $6s$ shells in addition to combined triple excitations involving those shells and the $5d$ shell. These excitations lead to a decrease of α_{SM} on the absolute by about 6%, which is significantly greater than the corresponding correction for Xe. Accounting for such types of quadruple excitations in the expansion is computationally too expensive, but from the understanding of the general effects we can predict that their inclusion would lead to a further (absolute) decrease of α_{SM} on the order of a few percent only, due to increasing energy denominators in a perturbative picture.

We, therefore, obtain our final value from a base value with the largest number of correlated electrons (SD34) improved by a correction for higher combined excitations (triples and quadruples) from the valence and the outer core shells, according to

$$\begin{aligned}&\alpha_{\text{SM}}(\text{Final})\\&\quad=\alpha_{\text{SM}}(\text{SD34/20au})\\&\qquad+\alpha_{\text{SM}}(\text{SD10\_SDT12/20au})-\alpha_{\text{SM}}(\text{SD12/20au})\\&\qquad+\alpha_{\text{SM}}(\text{SD10\_SDTQ12/5au})-\alpha_{\text{SM}}(\text{SD10\_SDT12/5au})\\&\qquad+\alpha_{\text{SM}}(\text{SD10\_SDT20/10au})-\alpha_{\text{SM}}(\text{SD10\_SDT12/10au}).\end{aligned}$$

The first of these two corrections—the one due to combined triple excitations—amounts to 6.8% of the DCHF value. The second—due to combined quadruple excitations—amounts to 2.4% of the DCHF value. No higher excitations from the valence shells make a contribution larger than about 0.3%.

The uncertainty estimate for Hg results from adding individual uncertainties for the nuclear density model (3%), the atomic basis set (2%), the higher excitation ranks (4%), and the Breit interaction (1%).

Including estimated uncertainties our final result is in agreement with earlier CI + MBPT calculations by Dzuba *et al.* as well as with coupled-cluster calculations by Singh *et al.* and Latha *et al.* and the MCDF calculation by Radžiūtė *et al.* The most recent other high-level calculation by Sahoo *et al.* disagrees with all of these results.

A closer look at the results in Table I of Sahoo and Das [48] reveals an inconsistency: When taking the combined power k of the operators $T^{(0)}$ and $T^{(0)\dagger}$ to infinity in Eq. (13) *ibidem* only a small correction (around −1.3%) to the dipole polarizability of Hg is observed compared to the calculation with $k = 5$, which is physically reasonable. However, for the nuclear Schiff moment interaction this correction amounts to 12% and for the $\mathcal{P},\mathcal{T}$-violating tensor-pseudotensor (T-PT) interaction even to more than 20%. The final result for the T-PT interaction in Ref. [48] also stands in stark disaccord with the result for the T-PT interaction in Ref. [49] and with the literature results cited therein.

D. TlF

Both in Ref. [28] and in our present work a careful and extensive optimization of atomic Gaussian basis sets for the Tl atom in TlF has been carried out. As can be seen in Table V, the DCHF result for our final sp-densified+1sp QZ-69s63p basis set differs from the corrected literature result of Quiney *et al.* [21,28] by only 2.2%. We consider this agreement as a further confirmation of the reliability of our technique of basis-set optimization. The DCHF result obtained by Skripnikov *et al.* [53] is within about 4% of the result obtained by Quiney *et al.* [28].

In Table VI we compile correlated Schiff moment interactions for TlF using various CI models. The main correction to the DCHF result comes from valence correlations among the $6s$ (Tl) and $2p$ (F) electrons (model SD8), quenching the interaction constant by nearly 9%. Full triple excitations out of these shells further reduce the value by almost 2% and in addition by a similar amount when a leading set of quadruple exci-

TABLE V. Molecular Schiff moment interaction constant for TlF calculated at the Hartree-Fock level including the core contribution with Gaussian nuclear density [37] at $R = 3.94$ a.u. [54] for studying electronic-basis-set convergence. Augmented basis sets are built from Dyall's QZ set including diffuse and correlating functions.

Model	W_{SM}(Tl) (a.u.)	ε_{DCHF} (a.u.)
QZ-34s31p	42877	−20374.47704191
sp-densified QZ-67s61p	30737	−20374.47575145
***sp*-densified+*1sp*QZ-69s63p**	**45419**	−20374.47660904
sp-densified+2*sp* QZ-71s65p	45540	−20374.47660743
sp-densified+3*sp* QZ-73s67p	45584	−20374.47660800
sp-densified+4*sp* QZ-75s69p	45602	−20374.47660786
sp-densified+5*sp* QZ-77s71p	45578	−20374.47660735
sp-densified+6*sp* QZ-79s73p	45594	−20374.47660803
sp-densified+7*sp* QZ-81s75p	45602	−20374.47660837
sp-densified+8*sp* QZ-83s77p	45584	−20374.47660780
Quiney *et al.* [28] (DCHF)[a]	46444	
Skripnikov *et al.* [53] (DCHF)	48377	

[a]Value from Ref. [28] corrected in Ref. [21] for the use of a more accurate operator for the Schiff moment interaction.

tations is added to the expansion, model 0.8auSDTQ8_SDT8 (where up to four particles are allowed in shells below an energy cutoff of 0.8 a.u.). Correlation contributions from the shells 1*s* and 2*s* (F) and 5*s* and 5*p* (Tl) are seen to be small, amounting to an increase of W_{SM} by only about 1.5%.

For TlF we obtain our final best result from a base value obtained with the model cvQZ+/SDT10_10au and adding corrections for quadruple excitations from the valence shells, correlation contributions from 1*s* (F) and 5*s*, 5*p* (Tl) shells, and a cutoff correction for the valence shell correlations, according to

$$\begin{aligned} W_{SM}(\text{Final}) &= W_{SM}(\text{cvQZ+/SDT10\_10au}) \\ &\quad + W_{SM}(\text{cvQZ+/0.8auSDTQ8\_SDT8\_5.5au}) \\ &\quad - W_{SM}(\text{cvQZ+/SDT8\_5.5au}) \\ &\quad + W_{SM}(\text{cvQZ+/SD20\_10au}) - W_{SM}(\text{cvQZ+/SD10\_10au}) \\ &\quad + W_{SM}(\text{cvQZ+/SD8\_40au}) - W_{SM}(\text{cvQZ+/SD8\_10au}). \end{aligned}$$

The uncertainty estimate for TlF results from adding individual uncertainties for the nuclear density model (3%), the atomic basis set (2%), the higher excitation ranks (2%), the innershell correlations (1%), and the Breit interaction (1%).

Our final best result is in agreement with both the operator-shifted results from Ref. [29] by Flambaum *et al.* in Ref. [21] and the recent CCSD(T) calculation by Skripnikov *et al.* [53]. The calculation by Abe *et al.* [56] uses an older form of the Schiff moment interaction operator. If scaled in the way the result obtained by Petrov *et al.* [29] has been corrected in Ref. [21], then the result would end up fairly close to the CCSD(T) result obtained by Skripnikov *et al.* [53]. Thus, for TlF all high-level-correlated many-body calculations yield values in accord with each other for the Schiff moment interaction.

TABLE VI. Molecular Schiff moment interaction constant for the thallium nucleus in TlF including electron correlation effects and the core contribution using the Dyall-cvQZ-69s63p basis set (denoted cvQZ+ in the Table) and a Gaussian nuclear density [37] at $R = 3.94$ a.u. [55].

Basis set/Model	W_{SM}(Tl) (a.u.)
cvQZ/DCHF	42877
cvQZ+/DCHF	45419
cvQZ+/SD8_5.5au	40779
cvQZ+/SD8_10au	41198
cvQZ+/SD8_20au	41431
cvQZ+/SD8_40au	41438
cvQZ+/SDT8_5.5au	39954
cvQZ+/SDT8_10au	40314
cvQZ+/SDT8_20au	40495
cvQZ+/0.8auSDTQ8_SDT8_5.5au	38863
cvQZ+/SD10_10au	41584
cvQZ+/SDT10_10au	40544
cvQZ+/SD16_10au	41762
cvQZ+/SD18_10au	41838
cvQZ+/SD20_10au	41858
Final present	**39967±3600**
Flambaum *et al.* [21,29] (operator-shifted CC)	40539
Skripnikov *et al.* [53] [CCSD(T)]	37192
Abe *et al.* [56] (CC)	41136

IV. CONCLUSIONS

Using the $\mathcal{P},\mathcal{T}$-violating energy shift $\Delta\varepsilon$ from the most recent measurements on the present systems and our calculated interaction constants we can determine the nuclear Schiff moment S itself, in the context of a single-source assumption. It results from the relation

$$\Delta\varepsilon = 2W_{SM}S, \tag{21}$$

where using our final central value for W_{SM} from Table VI and the measured frequency shift of $(1.4 \pm 2.4) \times 10^{-4}$ Hz from Ref. [30] yields

$$S(^{205}\text{Tl}) = (3.9 \pm 6.8) \times 10^{-11}\, e\,\text{fm}^3 \tag{22}$$

for the Schiff moment of the ^{205}Tl nucleus. The CENTREX Collaboration [20] aims at a significant increase in sensitivity to hadronic $\mathcal{T}$-violating fundamental interactions which—combined with the recent results for W_{SM}—will lead to stronger constraints on the nuclear Schiff moment in the case of a null measurement with tighter uncertainties.

The limit on the nuclear Schiff moment can be used to infer limits on the CPV pion-nucleon couplings, the QCD Θ parameter, and chromo-EDMs following the relations in Ref. [21].

A stronger constraint than the one in Eq. (22) can be placed on the Schiff moment of the ^{199}Hg nucleus. Using the upper bound on the Hg EDM of

$$|d_{\text{Hg}}| < 7.4 \times 10^{-30}\, e\,\text{cm} \tag{23}$$

from Ref. [26] and our central value for the Schiff moment interaction from Table IV yields an upper bound to the Hg

TABLE VII. Atomic Schiff moment interaction constant α_{SM} for Xe calculated at the Hartree-Fock level including the core contribution with Gaussian nuclear density [37] for studying electronic-basis-set convergence using several s- and p-space densifications and the addition of denser and more diffuse (s, p) function pairs. E_{ext} is set to 0.0003 a.u. Augmented basis sets are built from Dyall's QZ with diffuse and correlating functions. $+1sp$ means one denser s and p function; one more diffuse s and p function has been added to the basis set.

Model	(s, p) space	α_{SM} $(10^{-17}\frac{e\,\mathrm{cm}}{e\,\mathrm{fm}^3})$	ε_{DCHF} (a.u.)
QZ	$34s28p$	0.318	−7446.895409376
QZ $+1sp$*	$36s30p$	0.369	−7446.895386026
Simple sp-densified QZ	$67s55p$	0.314	−7446.895379750
Simple sp-densified QZ$+1sp$	$69s57p$	0.373	−7446.895401869
Double sp-densified QZ	$133s109p$	0.362	−7446.895392349
Double sp-densified QZ$+1sp$	$135s111p$	0.359	−7446.895401000
Double sp-densified QZ$+2sp$	$137s113p$	0.354	−7446.895401764
Double sp-densified QZ$+3sp$	$139s115p$	0.369	−7446.895401848
Double sp-densified QZ$+4sp$	$141s117p$	0.372	−7446.895401815
Double sp-densified QZ$+5sp$	$143s119p$	0.375	−7446.895401836
Double sp-densified QZ$+6sp$	$145s121p$	0.376	−7446.895401842
Double sp-densified QZ$+7sp$	$147s123p$	0.375	−7446.895401832
Double sp-densified QZ$+8sp$	$149s125p$	0.376	−7446.895401826
Double sp-densified QZ$+9sp$	$151s127p$	0.376	−7446.895401837
Double sp-densified QZ$+10sp$	$153s129p$	0.376	−7446.895401813
Triple sp-densified QZ	$265s217p$	0.051	−7446.895394063
Triple sp-densified QZ$+1sp$	$267s219p$	0.684	−7446.895399110

Schiff moment:

$$|S_{Hg}| < 3.3 \times 10^{-13}\, e\,\mathrm{fm}^3. \tag{24}$$

This is the same value as the one proposed in Ref. [26] where an average over various uncorrelated and correlated Schiff moment interactions from the literature was used. In the present case a rigorously calculated interaction parameter α_{SM}(Hg) including the effects of interelectron correlations in the Hg atom ground state replaces that average value, which it happens to match. The nuclear Schiff moment of ^{129}Xe and ^{199}Hg has recently been calculated as a function of the strong π-meson-nucleon interaction constants [57]. Combined with these dependencies our results can be used to constrain these interaction constants and as a function of the nucleon EDMs [58].

TABLE VIII. Atomic Schiff moment interaction constant α_{SM} $(10^{-17}\frac{e\,\mathrm{cm}}{e\,\mathrm{fm}^3})$ for Xe calculated at the Hartree-Fock level including the core contribution with Gaussian nuclear density [37] for studying electronic-basis-set convergence by addition of denser (s, p) pairs versus addition of denser (s, p) and more diffuse (s, p) pairs. E_{ext} is set to 0.0003 a.u. Augmented basis sets are built from Dyall's QZ set with diffuse and correlating functions.

	Addition of (s, p) dense pairs			Addition of (s, p) dense/diffuse pairs		
Model	(s, p) space	α_{SM}	ε_{DCHF} (a.u.)	(s, p) space	α_{SM}	ε_{DCHF} (a.u.)
QZ	$34s28p$	0.318	−7446.895409376	$34s28p$	0.318	−7446.895409376
QZ$+1sp$	$35s29p$	0.368	−7446.895385894	$36s30p$	0.369	−7446.895386026
QZ$+2sp$	$36s30p$	0.369	−7446.895384072	$38s32p$	0.369	−7446.895384244
QZ$+3sp$	$37s31p$	0.369	−7446.895383784	$40s34p$	0.370	−7446.895383956
QZ$+4sp$	$38s32p$	0.369	−7446.895383738	$42s36p$	0.371	−7446.895383915
QZ$+5sp$	$39s33p$	0.371	−7446.895383742	$44s38p$	0.370	−7446.895383987
QZ$+6sp$	$40s34p$	0.370	−7446.895383941	$46s40p$	0.370	−7446.895384141
QZ$+7sp$	$41s35p$	0.370	−7446.895383410	$48s42p$	0.372	−7446.895384163
QZ$+8sp$	$42s36p$	0.370	−7446.895383571	$50s44p$	0.376	−7446.895382476
sp-densified QZ	$67s55p$	0.314	−7446.895379750	$67s55p$	0.314	−7446.895379750
sp-densified QZ$+1sp$	$68s56p$	0.378	−7446.895401868	$69s57p$	0.373	−7446.895401869
sp-densified QZ$+2sp$	$69s57p$	0.375	−7446.895401802	$71s59p$	0.375	−7446.895401810
sp-densified QZ$+3sp$	$70s58p$	0.376	−7446.895401801	$73s61p$	0.375	−7446.895401762
sp-densified QZ$+4sp$	$71s59p$	0.376	−7446.895401801	$75s63p$	0.375	−7446.895401779
sp-densified QZ$+5sp$	$72s60p$	0.378	−7446.895401802	$77s65p$	0.376	−7446.895401790
sp-densified QZ$+6sp$	$73s61p$	0.375	−7446.895401802	$79s67p$	0.375	−7446.895401745
sp-densified QZ$+7sp$	$74s62p$	0.375	−7446.895401799	$81s69p$	0.374	−7446.895401770
sp-densified QZ$+8sp$	$75s63p$	0.376	−7446.895401800	$83s71p$	0.375	−7446.895401790

ACKNOWLEDGMENTS

We thank Vladimir Dzuba (Sydney) for numerous helpful discussions and for sharing details of his calculations with us.

APPENDIX

Tables VII and VIII give details on the basis-set optimization for Xe.

[1] S. L. Glashow, Partial-symmetries of weak interactions, Nuc. Phys. **22**, 579 (1961).

[2] S. Weinberg, A Model of Leptons, Phys. Rev. Lett. **19**, 1264 (1967).

[3] A. Salam, Weak and electromagnetic interactions, Conf. Proc. C **680519**, 367 (1968).

[4] G. Hinshaw *et al.*, Nine-year Wilkinson microwave anisotropy probe (WMAP) observations: cosmological parameter results, Astrophys. J. Suppl. **208**, 19 (2013).

[5] M. Dine and A. Kusenko, Origin of the matter-antimatter asymmetry, Rev. Mod. Phys. **76**, 1 (2003).

[6] A. D. Sakharov, Violation of CP invariance, C asymmetry, and baryon asymmetry of the universe, JETP Lett. **5**, 24 (1967).

[7] J. H. Christenson, J. W. Cronin, V. L. Fitch, and R. Turlay, Evidence for the 2π Decay of the K_2^0 Meson, Phys. Rev. Lett. **13**, 138 (1964).

[8] P. Villanueva-Pérez, Direct observation of time.reversal violation in B mesons at BABAR, J. Phys.: Conf. Ser. **447**, 012024 (2013).

[9] K. Abe *et al.*, Observation of Large CP Violation in the Neutral *B* Meson System, Phys. Rev. Lett. **87**, 091802 (2001).

[10] M. Kobayashi and T. Maskawa, CP violation in the renormalizable theory of weak interaction, Prog. Theor. Phys. **49**, 652 (1973).

[11] M. Raidal *et al.*, Flavor physics of leptons and dipole moments, Eur. Phys. J. C **57**, 13 (2008).

[12] W. Pauli, Editor, *Exclusion Principle, Lorentz Group and Reflection of Space-Time and Charge* (McGraw-Hill, New York, 1955), pp. 30–51.

[13] B. Pontecorvo, Inverse beta processes and nonconservation of lepton charge, Zh. Eksp. Teor. Fiz. **34**, 247 (1957).

[14] R. Alarcon *et al.*, Electric dipole moments and the search for new physics, arXiv:2203.08103.

[15] V. Cirigliano, M. J. Ramsey-Musolf, and U. van Kolck, Low energy probes of physics beyond the standard model, Prog. Part. Nucl. Phys. **71**, 2 (2013).

[16] M. Pospelov and A. Ritz, Electric dipole moments as probes of new physics, Ann. Phys. **318**, 119 (2005).

[17] T. Chupp, P. Fierlinger, M. J. Ramsey-Musolf, and J. T. Singh, Electric dipole moments of atoms, molecules, nuclei, and particles, Rev. Mod. Phys. **91**, 015001 (2019).

[18] A. Shindler, Flavor-diagonal CP violation: the electric dipole moment, Eur. Phys. J. D **57**, 128 (2021).

[19] M. D. Swallows, T. H. Loftus, W. C. Griffith, B. R. Heckel, E. N. Fortson, and M. V. Romalis, Techniques used to search for a permanent electric dipole moment of the ^{199}Hg atom and the implications for *CP* violation, Phys. Rev. A **87**, 012102 (2013).

[20] O. Grasdijk, O. Timgren, J. Kastelic, T. Wright, S. Lamoreaux, D. DeMille, K. Wenz, M. Aitken, T. Zelevinsky, T. Winick, and D. Kawall, CENTREX: A new search for time-reversal symmetry violation in the ^{205}Tl nucleus, Quantum Sci. Technol. **6**, 044007 (2021).

[21] V. V. Flambaum, V. A. Dzuba, and H. B. Tran Tan, Time- and parity-violating effects of the nuclear Schiff moment in molecules and solids, Phys. Rev. A **101**, 042501 (2020).

[22] I. B. Khriplovich and S. K. Lamoreaux, *CP Violation Without Strangeness* (Springer, Berlin, 1997).

[23] V. Spevak, N. Auerbach, and V. V. Flambaum, Enhanced T-odd, P-odd electromagnetic moments in reflection asymmetric nuclei, Phys. Rev. C **56**, 1357 (1997).

[24] S. M. Barr, T- and P-odd electron-nucleon interactions and the electric dipole moments of large atoms, Phys. Rev. D **45**, 4148 (1992).

[25] T. Fleig and M. Jung, Model-independent determinations of the electron EDM and the role of diamagnetic atoms, J. High Energy Phys. 07 (2018) 012.

[26] B. Graner, Y. Chen, E. G. Lindahl, and B. R. Heckel, Reduced Limit on the Permanent Electric Dipole Moment of ^{199}Hg, Phys. Rev. Lett. **116**, 161601 (2016).

[27] V. V. Flambaum and V. A. Dzuba, Electric dipole moments of atoms and molecules produced by enhanced nuclear Schiff moments, Phys. Rev. A **101**, 042504 (2020).

[28] H. M. Quiney, J. K. Lærdahl, T. Saue, and K. Fægri, Jr., *Ab initio* Dirac-Hartree-Fock calculations of chemical properties and PT-odd effects in thallium fluoride, Phys. Rev. A **57**, 920 (1998).

[29] A. N. Petrov, N. S. Mosyagin, T. A. Isaev, A. V. Titov, V. F. Ezhov, E. Eliav, and U. Kaldor, Calculation of P,T-Odd Effects in ^{205}TlF Including Electron Correlation, Phys. Rev. Lett. **88**, 073001 (2002).

[30] D. Cho, K. Sangster, and E. A. Hinds, Search for time-reversal-symmetry violation in thallium fluoride using a jet source, Phys. Rev. A **44**, 2783 (1991).

[31] V. V. Flambaum and J. S. M. Ginges, Nuclear Schiff moment and time-invariance violation in atoms, Phys. Rev. A **65**, 032113 (2002).

[32] V. A. Dzuba, V. V. Flambaum, J. S. M. Ginges, and M. G. Kozlov, Electric dipole moments of Hg, Xe, Rn, Ra, Pu, and TlF induced by the nuclear Schiff moment and limits on time-reversal violating interactions, Phys. Rev. A **66**, 012111 (2002).

[33] T. Fleig and L. V. Skripnikov, P,T-violating and magnetic hyperfine interactions in atomic thallium, Symmetry **12**, 498 (2020).

[34] S. Knecht, H. J. Aa. Jensen, and T. Fleig, Large-scale parallel configuration interaction. II. Two- and four-component double-group general active space implementation with application to BiH, J. Chem. Phys. **132**, 014108 (2010).

[35] T. Fleig, J. Olsen, and C. M. Marian, The generalized active space concept for the relativistic treatment of electron correlation. I. Kramers-restricted two-component configuration interaction, J. Chem. Phys. **114**, 4775 (2001).

[36] T. Fleig, J. Olsen, and L. Visscher, The generalized active space concept for the relativistic treatment of electron correlation. II: Large-scale configuration interaction implementation based on

relativistic 2- and 4-spinors and its application, J. Chem. Phys. **119**, 2963 (2003).

[37] L. Visscher and K. G. Dyall, Dirac-Fock atomic electronic structure calculations using different nuclear charge distributions, At. Data Nucl. Data Tables **67**, 207 (1997).

[38] K. G. Dyall, Relativistic double-zeta, triple-zeta, and quadruple-zeta basis sets for the 4s, 5s, 6s, and 7s elements, J. Phys. Chem. A **113**, 12638 (2009); Basis sets are available from the Dirac web site, http://dirac.chem.sdu.dk.

[39] K. G. Dyall, Relativistic double-zeta, triple-zeta, and quadruple-zeta basis sets for the 4p, 5p and 6p elements, Theoret. Chim. Acta **115**, 441 (2006).

[40] K. Fægri and K. G. Dyall, *Basis sets for relativistic calculations, in Relativistic Electronic Structure Theory*, edited by P. Schwerdtfeger (Elsevier, Amsterdam, 2002), Vol. 1, Chap. 5, p. 259.

[41] T. Saue *et al.*, The DIRAC code for relativistic molecular calculations, J. Phys. Chem. **152**, 204104 (2020).

[42] R. E. Stanton and S. Havriliak, Kinetic balance: A partial solution to the problem of variational safety in Dirac calculations, J. Chem. Phys. **81**, 1910 (1984).

[43] S. M. Ramachandran and K. V. P. Latha, Core-polarization studies of nuclear-Schiff-moment-induced permanent electric dipole moments of atomic ^{129}Xe, ^{171}Yb, and ^{225}Ra, Phys. Rev. A **90**, 042503 (2014).

[44] A. Sakurai, B. K. Sahoo, K. Asahi, and B. P. Das, Relativistic many-body theory of the electric dipole moment of ^{129}Xe and its implications for probing new physics beyond the standard model, Phys. Rev. A **100**, 020502(R) (2019).

[45] V. A. Dzuba, V. V. Flambaum, and S. G. Porsev, Calculations of the (P, T)-odd electric dipole moments for the diamagnetic atoms ^{129}Xe, ^{171}Yb, ^{199}Hg, ^{211}Rn, and ^{225}Ra, Phys. Rev. A **80**, 032120 (2009).

[46] Y. Singh, B. K. Sahoo, and B. P. Das, *Ab initio* determination of the P- and T-violating coupling constants in atomic Xe by the relativistic-coupled-cluster method, Phys. Rev. A **89**, 030502(R) (2014); Erratum: *Ab initio* determination of the P- and T-violating coupling constants in atomic Xe by the relativistic-coupled-cluster method [Phys. Rev. A 89, 030502(R) (2014)], **90**, 039903(E) (2014).

[47] V. Dzuba (private communication, 2021).

[48] B. K. Sahoo and B. P. Das, Relativistic Normal Coupled-Cluster Theory for Accurate Determination of Electric Dipole Moments of Atoms: First Application to the ^{199}Hg Atom, Phys. Rev. Lett. **120**, 203001 (2018).

[49] T. Fleig, $\mathcal{P}$, $\mathcal{T}$-odd tensor-pseudotensor interactions in atomic ^{199}Hg and ^{225}Ra, Phys. Rev. A **99**, 012515 (2019).

[50] K. V. P. Latha, D. Angom, B. P. Das, and D. Mukherjee, Probing *CP* Violation with the Electric Dipole Moment of Atomic Mercury, Phys. Rev. Lett. **103**, 083001 (2009); Erratum: Probing CP Violation with the Electric Dipole Moment of Atomic Mercury [Phys. Rev. Lett. **103**, 083001 (2009)], **115**, 059902(E) (2015).

[51] Y. Singh and B. K. Sahoo, Rigorous limits for hadronic and semi-leptonic *CP*-violating coupling constants from the electric dipole moment of ^{199}Hg, Phys. Rev. A **91**, 030501(R) (2015).

[52] L. Radžiūtė, G. Gaigalas, P. Jönsson, and J. Bieroń, Electric dipole moments of superheavy elements: A case study on copernicium, Phys. Rev. A **93**, 062508 (2016).

[53] L. V. Skripnikov, N. S. Mosyagin, A. V. Titov, and V. V. Flambaum, Actinide and lanthanide molecules to search for strong CP-violation, Phys. Chem. Chem. Phys. **22**, 18374 (2020).

[54] K. P. Huber and G. Herzberg, *Molecular Spectra and Molecular Structure* (Van Nostrand Reinhold, New York, 1979).

[55] K. P. Huber and G. H. Herzberg, Constants of diatomic molecules (data prepared by Jean W. Gallagher and Russell D. Johnson, III), in *NIST Chemistry WebBook, NIST Standard Reference Database Number 69*, edited by P. J. Linstrom and W. G. Mallard, National Institute of Standards and Technology, Gaithersburg, MD, https://doi.org/10.18434/T4D303 (retrieved February 2, 2022).

[56] M. Abe, T. Tsutsui, J. Ekman, M. Hada, and B. P. Das, Accurate determination of the enhancement factor X for the nuclear Schiff moment in ^{205}TlF molecule based on the four-component relativistic coupled-cluster theory, Mol. Phys. **118**, e1767814 (2020).

[57] K. Yanase and N. Shimizu, Large-scale shell-model calculations of nuclear Schiff moments of ^{129}Xe and ^{199}Hg, Phys. Rev. C **102**, 065502 (2020).

[58] K. Yanase, Screening of nucleon electric dipole moments in atomic systems, Phys. Rev. C **103**, 035501 (2021).